

Free Vibration Analysis of Rotating Clamped-Clamped Multi-Layered Cylindrical Shells Containing Functionally Graded Middle Layer

Ehaab W. Jarallah
 Mechanical Engineering Dep.
 University of Anbar
 Al-Ramadi, Anbar, IRAQ
ehaabeng40@gmail.com

Hamad M. Hasan
 Mechanical Engineering Dep.
 University of Anbar
 Al-Ramadi, Anbar, IRAQ
hamadscience155@gmail.com

Khalid B. Najim
 Civil Engineering Dep.
 University of Anbar
 Al-Ramadi, Anbar, IRAQ
dr.khalid.najim@gmail.com

Received: 17-Aug.-2017 *Revised:* 25-Sep.-2017 *Accepted:* 04- Jan.-2018

<http://doi.org/10.29194/NJES21010153>

Abstract

The free vibration analysis of rotating multi-layered cylindrical shell is investigated based on the first order shear deformation theory (FSDT) of shell. Cylindrical shell consists of three layers; outer and inner layers are isotropic material and the middle layer is a functionally graded material (FGM). The material properties for middle layer are assumed to be graded in the thickness direction. Based on Hamilton's principle, the equilibrium equations and the equations of motion are derived and then solved by using the differential quadrature method (DQM) as a numerical tool. MATLAB software was adopted for programming the equations and the related boundary condition. The effect of (FGM) layer thickness, angular speed, index power law, circumferential wave number on the natural frequency of the clamped-clamped rotating cylindrical shell were examined. The numerical results showed that a reasonable agreement between the present study and analytical data available in the literature.

List of Symbols

English Symbols

Notation	Description
[C]	Damping matrix
{d}	Degrees of freedom
E	Young's modulus
\tilde{E}	Equivalence Young's modulus for cylindrical shell
G	Shear rigidity
H	Total thickness of the cylindrical shell
h	Thickness of middle layer
K	Kinetic energy
[\tilde{K}]	Equivalent stiffness matrix
k_s	Shear correction factor
L	Length of the cylindrical shell
[M]	Mass matrix
m	Circumferential wave number
N_x	Grid point in the longitudinal direction
p	Index power law
R	Mean radius of cylindrical shell

t	Time
t_1, t_2	Two arbitrary time
U	Strain energy
u, v, w	Displacement component at the reference surface
W	Work done
x, θ , z	Cylindrical coordinates

Greek Symbols

Notation	Description
δ	Mathematical operation called variation
ν	Poisson's ratio
ϵ	Normal strain component
γ	Shear strain component
σ	Stress component
$\varphi^x, \varphi^\theta$	Bending rotation of the cross section of the shell about θ and x-axis, respectively
ρ	Mass density
λ	Non-dimensional frequency parameter
ω_n	Natural frequency
Ω	Rotating velocity
Π	Total potential energy
$\frac{\partial(\)}{\partial(\)}$	Derivative with respect to specific axis

1. Introduction

Multi-layered rotating cylindrical shell is often used in mechanical, civil, electrical structures. The types of these structures vary from one application to other according to the function of this structure as well as the operating conditions. In recent years, a new class of engineering materials appeared called 'Functionally Graded Materials' (FGM) which is a mixture of two materials often ceramic and metal. With using FGM, the properties of structure can be enhanced and become more strength. Bayat et al. [1] studied the effect of mechanical and thermal loads on a functionally graded rotating disk according to first order shear deformation Mindlin plate and Von Karman theories. Malekzadeh et al. [2] used Hamilton's principle to derive the equations of motion depending on first order shear

deformation theory (FSDT) and examined the effect of the temperature increase on the frequency for the functionally graded circular arches in thermal environment. Malekzadeh [3] investigated the free vibration of functionally graded thick circular in thermal environment depending on the two dimensional elasticity theory. Li et al. [4] employed the Flügges shell theory to obtain the governing equations for simply supported three-layer cylindrical shell with functionally graded middle layer and tested the effect of material properties and geometrical parameters on natural frequency. Malekzadeh et al. [5] examined the free vibration of functionally graded circular curved beam in thermal environment by using the differential quadrature method (DQM) to solve the equations of motion. Dai and Zheng [6] used the Donnell shell theory to study buckling and post-buckling for laminated cylindrical shell with functionally graded layer. Malekzadeh and Heydarpour [7] studied the effect rotation on the vibration characteristics of a functionally graded (FG) cylindrical shell in thermal environment based on the first order shear deformation theory (FSDT). Shah et al. [8] investigated the vibration of three-layered cylindrical shell containing functionally graded layer in the middle and resting on elastic foundations. Malekzadeh et al. [9] studied the three-dimensional (3D) free vibration of truncated conical shell made of functionally graded material (FGM) in thermal environment. Malekzadeh and Heydarpour [10] investigated the effect of rotating speed, coriolis acceleration, geometry, material properties and different boundary conditions on the vibration characteristics for

functionally graded (FG) truncated conical shell. Naeem et al. [11] examined the vibration of three-layered cylindrical shell containing two functionally graded (FG) layer at inner and outer and the middle layer assumed isotropic material. Heydarpour et al. [12] calculated the natural frequency for rotating truncated conical shell based on the first order shear deformation theory (FSDT). Through the above, the free vibration of rotating multi-layered cylindrical shell with functionally graded (FG) middle layer have not been so fully investigated. Therefore, this research project focuses on the free vibration of rotating multi-layered cylindrical shell clamped at both ends and composed of three layer. Inner and outer layers will be in the form of isotropic material, while the middle layer in the form of functionally graded material (FGM).

2. Geometric model

A multi-layered cylindrical shell is schematically illustrated in Fig.1. Inner and outer as isotropic material and the middle layer as a functionally graded material (FGM). The geometrical parameters of cylindrical shell are: R is the mean radius, while H, h and L represent the shell thickness, thickness of middle layer and the length of the cylindrical shell, respectively. Ω is angular speed of the cylindrical shell spin around its axis. Cylindrical coordinates (x,θ,z) are used to describe the material points of the cylindrical shell in the middle undeformed plane, where x, θ and z are the axial, circumferential and the radial directions, respectively.

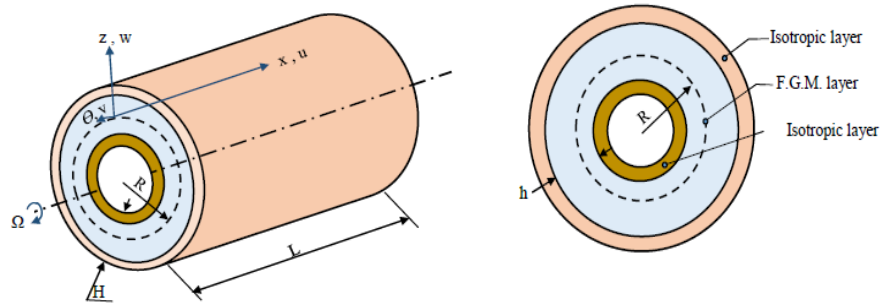


Figure 1: Detailed drawing of a rotating multi-layer cylindrical shell with functionally graded layer

3. Material properties:

For functionally graded material the Poisson's ratio assumed constant, while Young's modulus and density varies continuously in thickness directions (z. directions) depending on the simple power law distribution of materials. The Young's modulus for FG layer can be calculated as:

$$E(z) = E_m + (E_c - E_m) \left(\frac{2z+h}{2z} \right)^p \quad (1)$$

where E_c and E_m are values of outer surface (ceramic rich) and inner surface (metal rich) of

the functionally graded layer, p represents the power law index which is a positive real number [10] limited to $(0 \rightarrow \infty)$. The material properties of the three layers are presented in Tables (1,2).

4. Initial dynamic equilibrium equations:

Due to the rotation of the cylindrical shell, initial mechanical stresses are generated and then the effects of these stresses are taken in

consideration in the calculation of the free vibration. Referring to the theory of elasticity and according to the cylindrical coordinates, the linear strain – displacement relations [13] are :

$$\begin{aligned} \varepsilon_{0xx} &= \frac{\partial \bar{u}_0}{\partial x}, \varepsilon_{0\theta\theta} = \frac{\bar{w}_0}{(R+z)}, \varepsilon_{0zz} = \frac{\partial \bar{w}_0}{\partial z}, \\ \gamma_{0xz} &= \frac{\partial \bar{w}_0}{\partial x} + \frac{\partial \bar{u}_0}{\partial z} \end{aligned} \quad (2a-d)$$

The linear stress – strain relations [13] are :

$$\sigma_{0xx} = \tilde{E}[\varepsilon_{0xx} + \nu \varepsilon_{0\theta\theta}], \sigma_{0\theta\theta} = \tilde{E}[\sigma_{0\theta\theta} + \nu \sigma_{0xx}], \sigma_{0xz} = k_s G \gamma_{0xz} \quad (3a-c)$$

Where: \tilde{E} is the equivalence Young's modulus for cylindrical shell

$$\tilde{E} = \left(\frac{E}{1-\nu^2}\right)_{in} + \left(\frac{E(z)}{1-\nu^2}\right)_{FG} + \left(\frac{E}{1-\nu^2}\right)_{out}$$

G is the shear rigidity

$$G = \left(\frac{E}{2(1+\nu)}\right)_{in} + \left(\frac{E(z)}{2(1+\nu)}\right)_{FG} + \left(\frac{E}{2(1+\nu)}\right)_{out}$$

k_s is the shear correction factor , and ν is the Poisson's ratio. The principle of virtual work is used to derive equilibrium equations with related boundary conditions. The total potential energy can be written as:

$$\Pi = U - W \quad (4)$$

Where, Π , U, and W are the total potential energy, Strain energy, and the work done, respectively. By applying the integration by-part method, a set of ordinary differential equations are obtained and then the initial stresses are calculated.

Table 1: Materials properties of inner and outer layer

Layer	Modulus of elasticity $E(N/m^2)$	Poisson ratio(ν)	Density $\rho(Kg/m^3)$
Inner (ceramic)	151E +09	0.3	5700
Outer(metal)	68.95E +09	0.3	2714.5

Table 2: Materials properties of (FGM) layer

FGM	Modulus of elasticity $E(N/m^2)$	Poisson ratio(ν)	Density $\rho(Kg/m^3)$
Zirconia	1.68E +11	0.3	5700
Nickel	2.05098E +11	0.3	8900

5. Free vibration equations

On the assumption that the free vibration of the shell happens about its dynamic equilibrium positioning (non-deformed plane), therefore, based on this hypothesis, displacement components are measured from this position. According to the first order shear deformation theory (FSDT) of shell, the general displacement components ($\hat{u}, \hat{v}, \hat{w}$) at an arbitrary material point (x, θ, z) in the thickness direction (z-direction) measured from the non-deformed plane are as follows :

$$\hat{u}(x, \theta, z, t) = u_0(x) + z\varphi_0^x(x) + u(x, \theta, t) + z\varphi^x(x, \theta, t) \quad (5a)$$

$$\hat{v}(x, \theta, z, t) = v(x, \theta, t) + z\varphi^\theta(x, \theta, t) \quad (5b)$$

$$\hat{w}(x, \theta, z, t) = w_0(x) + w(x, \theta, t) \quad (5c)$$

Where $\varphi^x(x, \theta, t)$ and $\varphi^\theta(x, \theta, t)$ are the bending rotation of the cross section of the shell about θ and x-axis, respectively. Hamilton's principle is employed in order to derive the equations of motion with the regarding boundary conditions,

$$\int_{t_1}^{t_2} (\delta K - \delta U) dt = 0 \quad (6)$$

Where, t_1 and t_2 are two arbitrary times, δ is the variational operator, K is the kinetic energy and U is the potential energy of the shell. In this section, the initial mechanical stresses of the equilibrium state are included in the equations of motion. In order to achieve this, the nonlinear strain - displacement relations in the cylindrical coordinate [14] are taken into account. So, the form of potential and kinetic energy equations are:

$$\begin{aligned} \delta U &= \int_0^{2\pi} \int_0^L \int_{-\frac{H}{2}}^{\frac{H}{2}} [(\sigma_{xx} + \sigma_{0xx})\delta \hat{\varepsilon}_{xx} + \\ &(\sigma_{\theta\theta} + \sigma_{0\theta\theta})\delta \hat{\varepsilon}_{\theta\theta} + (\sigma_{xz} + \sigma_{0xz})\delta \hat{\gamma}_{xz} + \\ &\sigma_{x\theta} \delta \hat{\gamma}_{x\theta} + \sigma_{\theta z} \delta \hat{\gamma}_{\theta z}] (R+z) dz dx d\theta \end{aligned} \quad (7)$$

$$\begin{aligned} \delta K &= \int_0^{2\pi} \int_0^L \int_{-\frac{H}{2}}^{\frac{H}{2}} \rho \left[\frac{\partial \hat{u}}{\partial t} \frac{\partial \delta \hat{u}}{\partial t} + \frac{\partial \hat{v}}{\partial t} \frac{\partial \delta \hat{v}}{\partial t} + \frac{\partial \hat{w}}{\partial t} \frac{\partial \delta \hat{w}}{\partial t} + \right. \\ &\Omega \left(\hat{w} \frac{\partial \delta \hat{v}}{\partial t} + \frac{\partial \hat{v}}{\partial t} \delta \hat{w} - \frac{\partial \hat{w}}{\partial t} \delta \hat{v} - \hat{v} \frac{\partial \delta \hat{w}}{\partial t} \right) + \\ &\left. \Omega^2 (\hat{v} \delta \hat{v} + \hat{w} \delta \hat{w}) \right] (R+z) dz dx d\theta \end{aligned} \quad (8)$$

In equation (7), components $[\sigma_{xx}, \sigma_{\theta\theta}, \sigma_{xz}, \sigma_{x\theta}, \sigma_{\theta z}]$ represent the dynamic stress parts as a result of the rotation of shell, $(\sigma_{0xx}, \sigma_{0\theta\theta}, \sigma_{0xz})$ are the nonzero initial mechanical stress parts due to the equilibrium state, $(\hat{\varepsilon}_{xx}, \hat{\varepsilon}_{\theta\theta})$ and $(\hat{\gamma}_{xz}, \hat{\gamma}_{x\theta}, \hat{\gamma}_{\theta z})$ represent the normal and shear Green's strain relations [14]. By substitution of equations (7) and (8) in equation

(6), then apply integration by-parts to obtain equations of motion with boundary conditions.

6. Solution Method

It is difficult to find an analytical solution to the equations that were derived in the previous section because of the coupling of equations. Therefore, numerical methods of analysis are used. In this paper, the differential quadrature method (DQM) employed to solve the differential equations as shown in Fig (6). The principle of this method is that the derivative of a function with respect to a coordinate direction is expressed as a linear weighted sum of all the functional values at all mesh points along that direction [15]. Then a system of linear algebraic equations is obtained, the equations of equilibrium can be easily solved by using a system of algebraic equations solver. The final form of free vibration equation can be written as :

$$[M]\{\ddot{d}\} + [C]\{\dot{d}\} + [K]\{d\} = \{0\} \quad (9)$$

Where $[M]$ is the mass matrix, $[C]$ is the damping matrix and $[K]$ is the equivalent stiffness matrix. Finally, the eigenvalues and the natural frequency (ω_n) can be calculated from equation (9).

7. Numerical results and discussion

In this part, numerical results for rotating clamped-clamped multi-layered cylindrical shell

is verified and compared with those found in the literature in order to examine the efficiency and accuracy of the differential quadrature method (DQM).

The boundary conditions of the cylindrical shell is clamped-clamped for both ends ($x=0$, $x=L$). Most of the results in this paper are presented as non-dimensional frequency parameter (λ) which is defined as follows:

$$\lambda = \omega_n R \sqrt{\frac{\rho(1-\nu^2)}{E}} \quad (10)$$

Convergence of the differential quadrature method (DQM) has been verified as shown in Table (3). It is clear that when using number of grid points in the longitudinal direction more than seventeen ($N_x > 17$), there is no change in the value of frequency parameter (λ). In other words, when using ($N_x \geq 17$) the results are more accurate.

The natural frequencies (Hz) of different values of the circumferential wave number were compared with other results in the literature to determine the accuracy of the solution. Table (4) shows the maximum percentage of error between the present study and the results the literature [8] is 3.3144%. This maximum error occurs, when using circumferential wave number equals 2.

Table 3: Convergence of the frequency parameters (λ) ($\Omega=500$ rad/sec. , $L/R=2.5$, $m=1$, $p=1$, $R=1m.$, $H/R=0.05$)

Grid point(N_x)	11	12	13	17	24	25
λ_1	0.0355	0.0023	0.0025	0.0019	0.0019	0.0019

Table 4: Comparison of natural frequencies (Hz) ($\Omega=0$ rad/sec. , $L/R=20$, $p=5$, $R=1m.$, $H/R=0.002$)

Circumferential wave number m	Natural frequencies (Hz) (present)	Shah et al. [8]	Percentage of error (%)
1	28.703	28.754	0.1773
2	9.364	9.685	3.3144
3	5.331	5.482	2.7544
4	6.357	6.272	1.3552
5	9.143	9.312	1.8148

Table 5: Comparison of natural frequencies (Hz) ($\Omega=0$ rad/sec. , $L/R=20$, $p=0.5$, $R=1m.$, $H/R=0.002$)

Circumferential wave number m	Natural frequencies (Hz) (present)	Naeem et al. [11]	Percentage of error (%)
1	34.0303	34.6722	1.8513
2	12.5907	12.1477	3.6467
3	7.8552	7.2610	8.1834
4	9.0282	9.0512	0.2541

Another investigation of the accuracy is introduced in Table (5), the natural frequencies (Hz) of a cylindrical shell are compared with the available data in the reference [11]. The maximum difference between proposed approach

and Naeem et al. [11] is 0.5942 Hz (percentage of error is 8.1834%), that happens with using circumferential wave number equals 3.

From both Tables (4, 5), It can be seen that a good agreement and accuracy between the present

study and natural frequencies those available in the literature. After showing the convergence and accuracy of the differential quadrature method (DQM), several parameters were studied to find their effect on the natural frequencies and frequency parameters of the rotating clamped-clamped multi-layered cylindrical shell with (FG) layer at middle. Fig (2) illustrates the effect of angular velocity on frequency parameters, it is observed that the frequency parameters increase with increasing angular velocity. In addition, the relationship between the circumferential wave number and the frequency parameter at a different angular velocity was examined and introduced in Fig (3), It is found that the frequency parameters decrease by increasing the circumferential wave number until the circumferential wave number reaching to value (3), then the frequency parameters increase with the increase of the circumferential wave number. The effect of the thickness to mean radius ratio (H/R) on the frequency parameters at two different values of angular velocity are presented in Fig (4). The natural frequency of the cylindrical shell of the two angular velocity ($\Omega=0$ rad/sec. and $\Omega=500$ rad/sec.) increases with increasing the thickness to mean radius ratio (H/R). Also, it is showed that the natural frequency values when the cylindrical shell under no rotation condition are higher than that in the case of high rotational velocity. Fig (5) shows the effect of the power law index on the frequency parameters. The results showed that the frequency parameters increase when the power law index is 0.5, while there is a decrease in the frequency parameters if the power index is more than 0.5 under different angular velocity condition. Finally, in Table (6) the effect of the thickness of the functionally graded material (FGM) layer on the frequency parameters is presented for high and low rotational speed. It

was observed that the frequency parameters increases by increasing the thickness of the functionally graded layer. This means that the performance of the structure can be improved and made more rigidity by increasing the thickness of the functionally graded material layer.

Table 6: Variation of frequency parameters (λ) together with different values of thickness of (FG) layer , where ($L/R=2.5$, $p=1$, $m=1$, $R=1m$, $H/R=0.1$).

Thickness of (FG) layer h (m)	λ_1 at ($\Omega=50$ rad/sec.)	λ_1 at ($\Omega=1000$ rad/sec.)
0.01	0.7583	1.9295
0.015	3.6927	1.9391
0.02	4.1640	4.453

8. Conclusion

According to the first order shear deformation theory (FSDT) the free vibration analysis of rotating multi-layered cylindrical shell contains functionally graded material (FGM) in the middle was investigated. The effect of the initial mechanical stresses generated by the rotation of the cylindrical shell was taken into account in this study. Several parameters were studied to demonstrate their effect on the natural frequency. The increase in the thickness of the FG layer leads to an increase in the frequency parameters. Also, the increase of angular velocity may lead to an increase or decrease in frequency parameter depending on the geometrical and material parameters. On the other hand, the power law index has a significant effect on the frequency parameters especially in high rotational speed, the highest value of the frequency parameters can be obtained at the lowest value of the power law index.

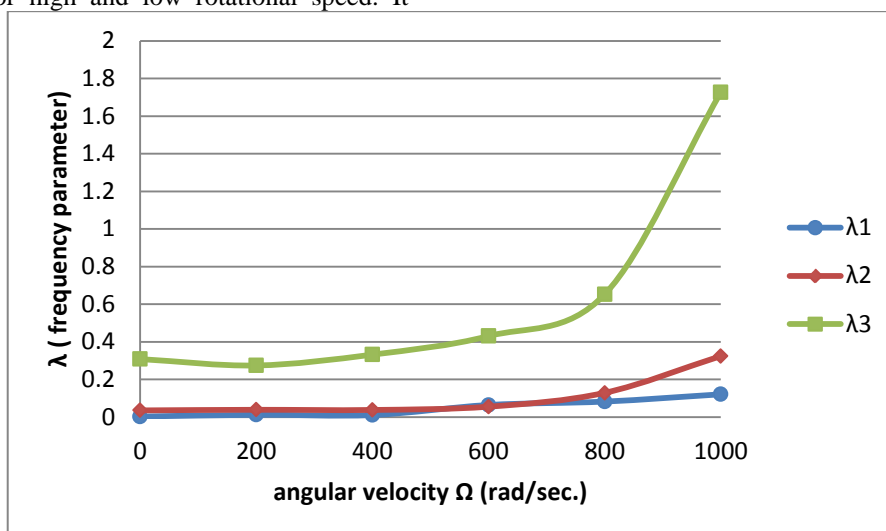


Figure 2 : Variation of frequency parameters (λ) with the angular velocity , Where ($p=1$, $L/R=2.5$, $m=1$, $R=1m$, $H/R=0.05$).

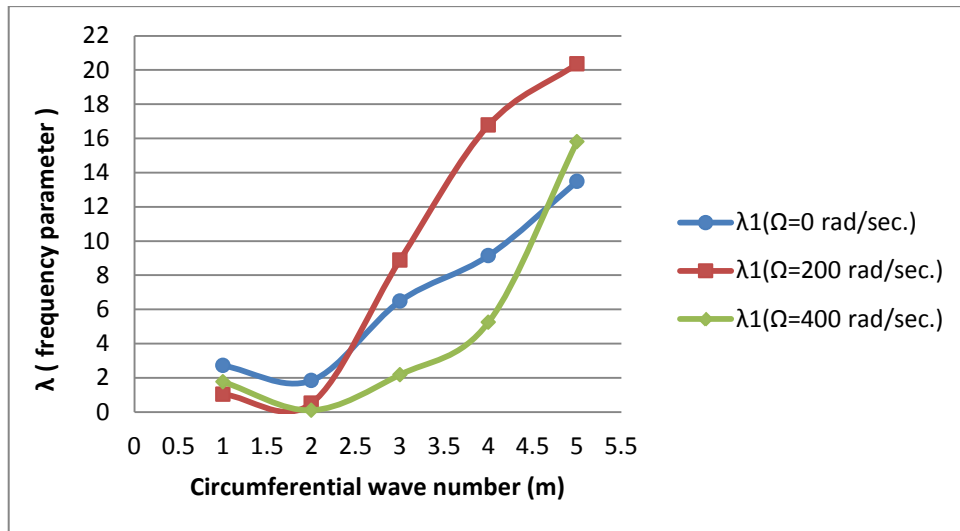


Figure 3: Variation of frequency parameters (λ) with the circumferential wave number(m), Where ($p=1$, $L/R=2.5$, $R=1\text{m}$, $H/R=0.05$).

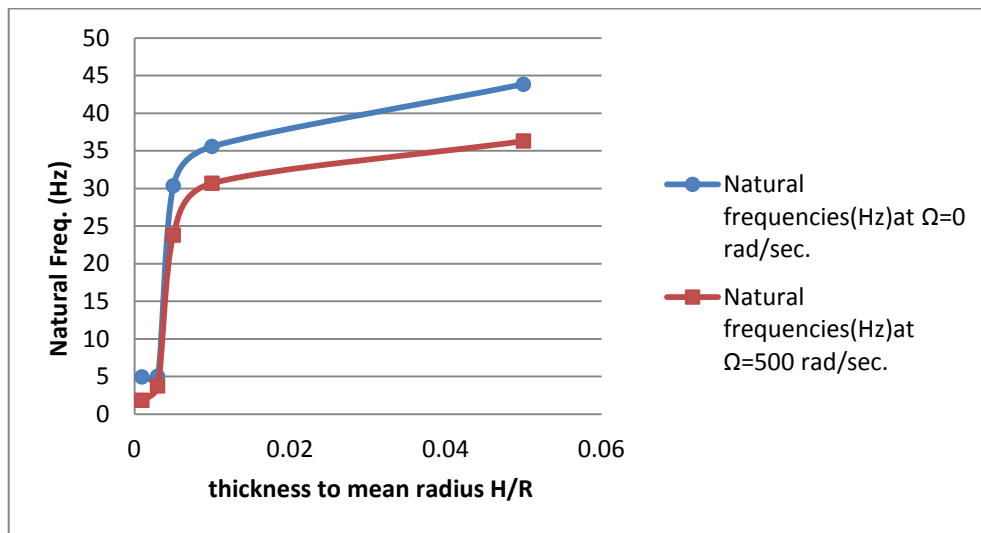


Figure 4: Variation of natural frequencies (Hz) together with (H/R) ratios, Where ($p=0.5$, $L/R=2.5$, $m=4$, $R=1\text{m}$).

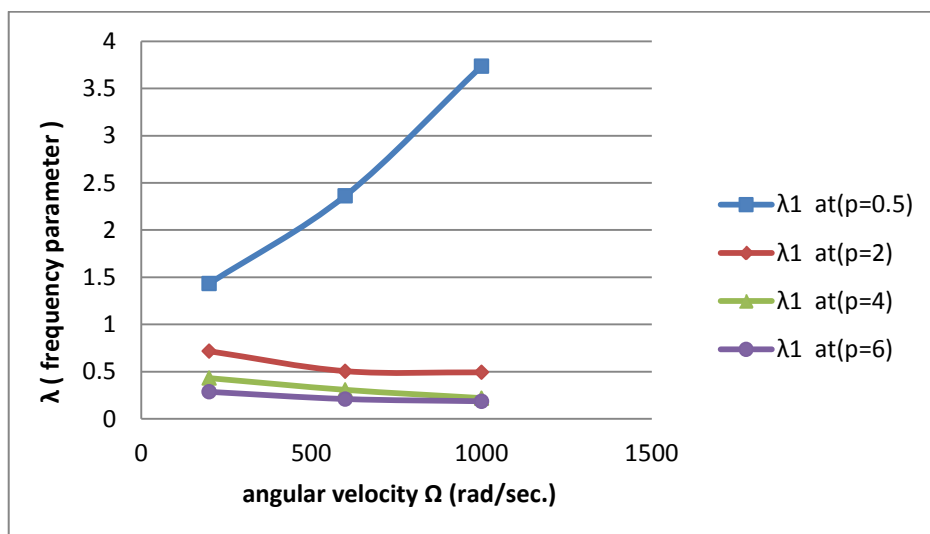


Figure 5: Variation of frequency parameters (λ) for different values of the power law index (p), Where ($L/R=2.5$, $m=1$, $R=1\text{m}$, $H/R=0.05$).

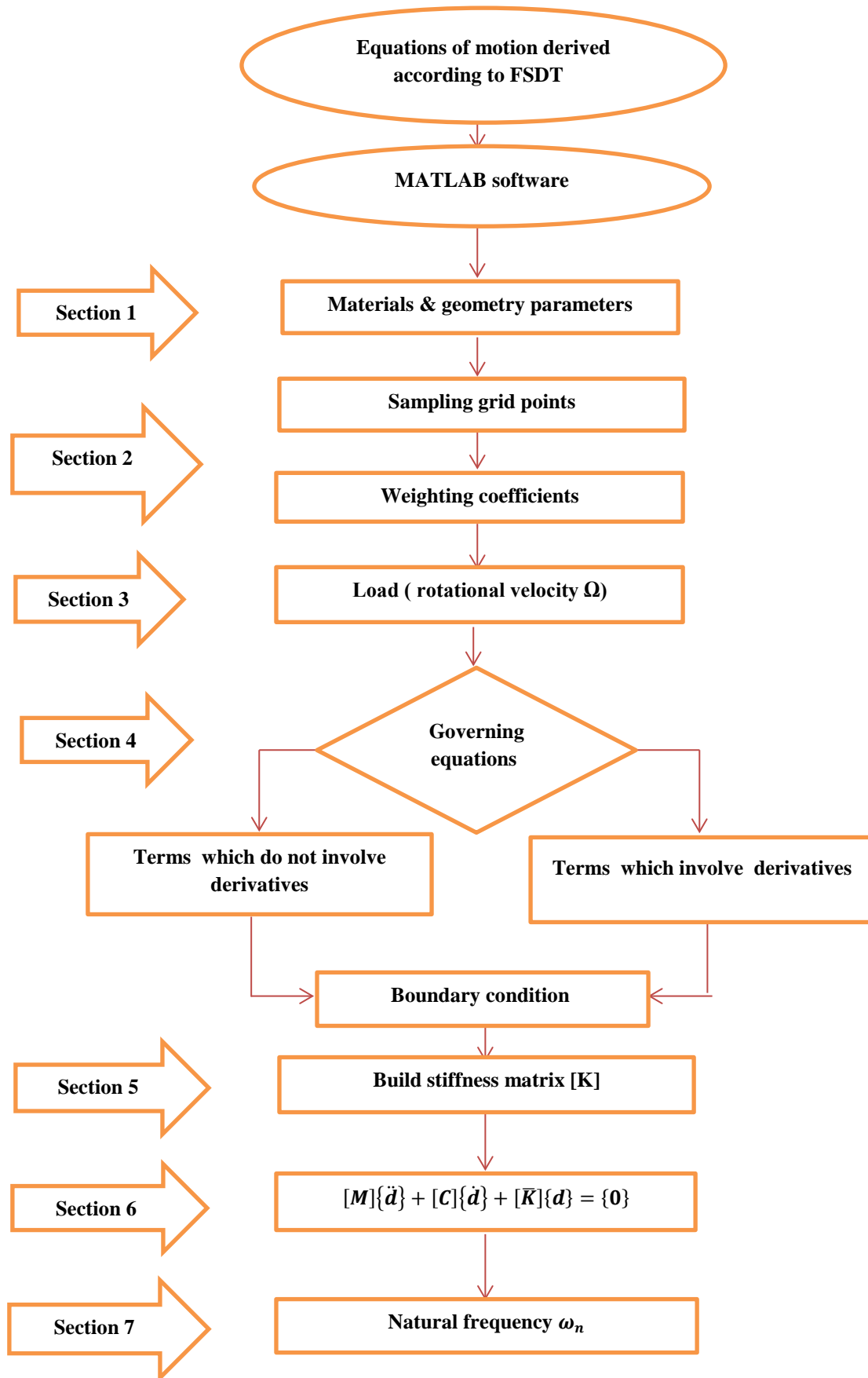


Figure 6: Flowchart illustrates solution algorithm in DQM

Appendix A

The nonlinear strain relations in the cylindrical coordinate system are [14] :

$$\begin{aligned} \epsilon_{xx} &= \frac{\partial u}{\partial x} + \frac{1}{2} \left[\left(\frac{\partial u}{\partial x} \right)^2 + \left(\frac{\partial v}{\partial x} \right)^2 + \left(\frac{\partial w}{\partial x} \right)^2 \right]. \\ \epsilon_{\theta\theta} &= \frac{1}{(R+z)} \left(\frac{\partial v}{\partial \theta} + w \right) + \frac{1}{2(R+z)^2} \left[\left(\frac{\partial w}{\partial \theta} - v \right)^2 + \left(\frac{\partial v}{\partial \theta} + w \right)^2 + \left(\frac{\partial u}{\partial \theta} \right)^2 \right]. \\ \epsilon_{zz} &= \frac{\partial w}{\partial z} + \frac{1}{2} \left[\left(\frac{\partial u}{\partial z} \right)^2 + \left(\frac{\partial v}{\partial z} \right)^2 + \left(\frac{\partial w}{\partial z} \right)^2 \right]. \\ \gamma_{\theta z} &= \frac{\partial v}{\partial z} + \frac{1}{(R+z)} \left(\frac{\partial w}{\partial \theta} - v \right) + \frac{1}{(R+z)} \left[\frac{\partial w}{\partial z} \left(\frac{\partial w}{\partial \theta} - v \right) + \frac{\partial v}{\partial z} \left(\frac{\partial v}{\partial \theta} + w \right) + \frac{\partial u}{\partial z} \frac{\partial u}{\partial \theta} \right]. \\ \gamma_{x\theta} &= \frac{\partial v}{\partial x} + \frac{1}{(R+z)} \frac{\partial u}{\partial \theta} + \frac{1}{(R+z)} \left[\frac{\partial w}{\partial x} \left(\frac{\partial w}{\partial \theta} - v \right) + \frac{\partial v}{\partial x} \left(\frac{\partial v}{\partial \theta} + w \right) + \frac{\partial u}{\partial x} + \frac{\partial u}{\partial \theta} \right]. \\ \gamma_{xz} &= \frac{\partial w}{\partial x} + \frac{\partial u}{\partial z} + \frac{\partial u}{\partial x} \frac{\partial u}{\partial z} + \frac{\partial v}{\partial x} \frac{\partial v}{\partial z} + \frac{\partial w}{\partial x} \frac{\partial w}{\partial z} . \end{aligned}$$

References

[1]. Bayat, M., M. Saleem, B.B. Sahari, A.M.S. Hamouda and E. Mahdi, *Thermo elastic analysis of a functionally graded rotating disk with small and large deflections*. Thin-Walled Structures, 2007. **45**(7): p. 677-691.
 [2]. Malekzadeh, P., M. Atashi, and G. Karami, *In-plane free vibration of functionally graded circular arches with temperature-dependent properties under thermal environment*. Journal of Sound and Vibration, 2009. **326**(3): p. 837-851.
 [3]. Malekzadeh, P., *Two-dimensional in-plane free vibrations of functionally graded circular arches with temperature-dependent properties*. Composite Structures, 2009. **91**(1): p. 38-47.
 [4]. Li, S.-R., X.-H. Fu, and R. Batra, *Free vibration of three-layer circular cylindrical shells with functionally graded middle layer*. Mechanics Research Communications, 2010. **37**(6): p. 577-580.
 [5]. Malekzadeh, P., M.G. Haghghi, and M. Atashi, *Out-of-plane free vibration of functionally graded circular curved beams in thermal*

environment. Composite Structures, 2010. **92**(2): p. 541-552.
 [6]. Dai, H.-L. and H.-Y. Zheng, *Buckling and post-buckling analyses for an axially compressed laminated cylindrical shell of FGM with PFRC in thermal environments*. European Journal of Mechanics-A/Solids, 2011. **30**(6): p. 913-923.
 [7]. Malekzadeh, P. and Y. Heydarpour, *Free vibration analysis of rotating functionally graded cylindrical shells in thermal environment*. Composite Structures, 2012. **94**(9): p. 2971-2981.
 [8]. Shah, A.G., A. Ali, M. N. Naeem and Sh. H. Arshad, *Vibrations of Three-Layered Cylindrical Shells with FGM Middle Layer Resting on Winkler and Pasternak Foundations*. Advances in Acoustics and Vibration, 2012. **2012**.
 [9]. Malekzadeh, P., A. Fiouze, and M. Sobhrouyan, *Three-dimensional free vibration of functionally graded truncated conical shells subjected to thermal environment*. International Journal of Pressure Vessels and Piping, 2012. **89**: p. 210-221.
 [10]. Malekzadeh, P. and Y. Heydarpour, *Free vibration analysis of rotating functionally graded truncated conical shells*. Composite Structures, 2013. **97**: p. 176-188.
 [11]. Naeem, M.N., A. Gul Khan, Sh. H. Arshad, A. G. Shah, M. Gamkhar, *Vibration of Three-Layered FGM Cylindrical Shells with Middle Layer of Isotropic Material for Various Boundary Conditions*. World Journal of Mechanics, 2014. **4**(11): p. 315.
 [12]. Heydarpour, Y., M. Aghdam, and P. Malekzadeh, *Free vibration analysis of rotating functionally graded carbon nanotube-reinforced composite truncated conical shells*. Composite Structures, 2014. **117**: p. 187-200.
 [13]. Fung, Y.-C., *Foundations of solid mechanics*. 1965: Prentice Hall.
 [14]. Saada, A.S., *Elasticity: theory and applications*. Vol. 16. 2013: Elsevier.
 [15]. Shu, C., *Differential quadrature and its application in engineering*. 2012: Springer Science & Business Media.

تحليل الاهتزاز الحر لأسطوانة دوارة متعددة الطبقات تحتوي على طبقة وسطى متدرجة الوظائف

خالد بتال نجم
 قسم الهندسة المدنية
 جامعة الانبار، العراق

حمد محمد حسن
 قسم الهندسة الميكانيكية
 جامعة الانبار، العراق

إيهاب وجيه جارالله
 قسم الهندسة الميكانيكية
 جامعة الانبار، العراق

الخلاصة:

وفقاً لنظرية التشوه القصي الاولي (FSDT) تم تحليل الاهتزاز الحر لأسطوانة متعددة الطبقات تحتوي على مادة متدرجة وظيفياً (FGM) في الوسط. الاسطوانة تتكون من ثلاث طبقات، الطبقتان الداخلية والخارجية مصنوعة من مواد متجانسة، بينما الطبقة الوسطى مصنوعة من مواد متدرجة وظيفياً تتغير خواصها خلال سمك الطبقة. تم اشتقاق معادلات التوازن ومعادلات الحركة باستخدام مبدأ هاميلتون ومن ثم تم حلها عددياً باستخدام طريقة التربيع التفاضلي (DQM). تم اعتماد برنامج الماتلاب في برمجة المعادلات وايجاد النتائج. تأثير سمك طبقة ال (FGM)، السرعة الزاوية وغيرها من المتغيرات على التردد الطبيعي للهيكل الاسطواني تم دراستها في هذا البحث. حيث اظهرت النتائج العددية توافق جيد عند مقارنتها مع نتائج تحليلية لدراسات سابقة.